YMTHE, Volume *25*

Supplemental Information

Gene Therapeutic Reversal of Peripheral Olfactory Impairment in Bardet-Biedl Syndrome

Corey L. Williams, Cedric R. Uytingco, Warren W. Green, Jeremy C. McIntyre, Kirill Ukhanov, Arthur D. Zimmerman, Dana T. Shively, Lian Zhang, Darryl Y. Nishimura, Val C. Sheffield, and Jeffrey R. Martens

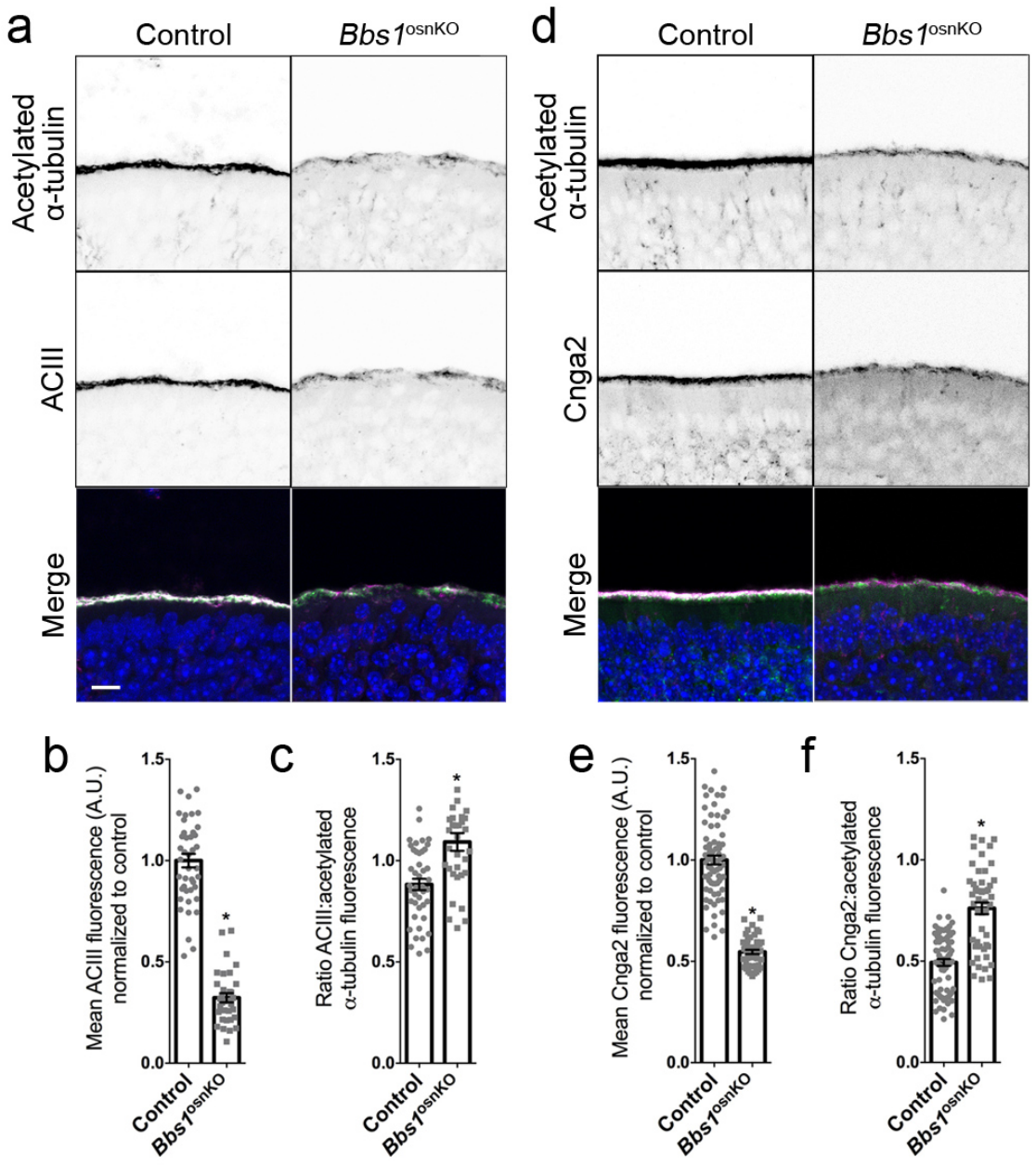
a
Control
Bbs1osnKO
Acetylated α-tubulin
ACIII
Merge
d
Control
Bbs1osnKO
Acetylated α-tubulin
Cnga2
Merge
b
Mean ACIII fluorescence (A.U.) normalized to control
1.5
1.0
0.5
0.0
*
Control
Bbs1osnKO
c
Ratio ACIII:acetylated α-tubulin fluorescence
1.5
1.0
0.5
0.0
*
Control
Bbs1osnKO
e
Mean Cnga2 fluorescence (A.U.) normalized to control
1.5
1.0
0.5
0.0
*
Control
Bbs1osnKO
f
Ratio Cnga2:acetylated α-tubulin fluorescence
1.5
1.0
0.5
0.0
*
Control
Bbs1osnKO

Fig. S1. Apical enrichment of ACIII and Cnga2 is retained in the OE of *Bbs1*^{osnKO} mutants. (*a*) Representative confocal images of coronal sections through olfactory epithelium of control and mutant mice, immunostained for (*top*) acetylated α-tubulin to reveal ciliary microtubules and (*middle*) adenylate cyclase 3 (ACIII). Compared (*left*) control, (*right*) *Bbs1*^{osnKO} tissue has diminished ACIII in the cilia layer on the apical surface of the OE. *(b*) Quantified data showing a significant reduction of ACIII fluorescence intensity in mutants versus controls. Student's t-test, * $p<0.0001$. (*c*) Quantified data showing changes to the ratio of ACIII to acetylated α-tubulin signal intensity at the apical OE surface in mutants versus controls. Student's t-test, * $p<0.0001$. (*d*) Representative confocal images of coronal sections through olfactory epithelium of control and mutant mice, immunostained for (*top*) acetylated α-tubulin and (*middle*) cyclic nucleotide-gated channel alpha 2 (Cnga2). Compared (*left*) control, (*right*) *Bbs1*^{osnKO} tissue has diminished Cnga2 in the cilia layer on the apical surface of the OE. *(e*) Quantified data showing a significant reduction of Cnga2 fluorescence intensity in mutants versus controls. Student's t-test, * $p<0.0001$. (*f*) Quantified data showing changes to the ratio of Cnga2 to acetylated α-tubulin signal intensity at the apical OE surface in mutants versus controls. Student's t-test, * $p<0.0001$. Values represent means ± SEM. Scale bar, 10 μm.

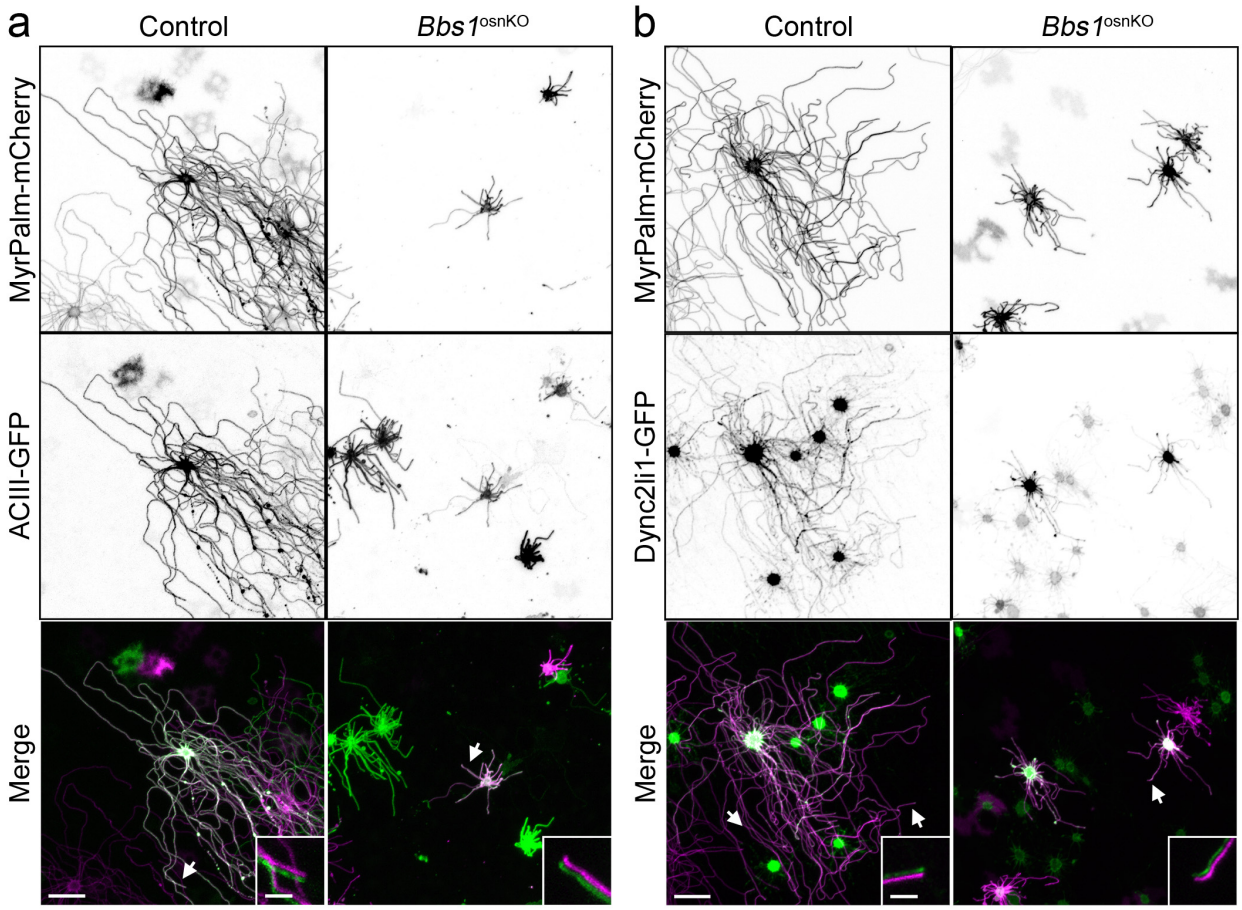

Fig. S2. OSN ciliation is diminished in *Bbs1*^{osnKO} mutants, but ACIII and Dync2li1 localization is unaffected. (*a*) Representative live *en face* images of ectopic (*top*) MyrPalm-mCherry and (*middle*) ACIII-GFP expression in olfactory epithelium of (*left*) control and (*right*) *Bbs1*^{osnKO} mice. Insets show magnified and color-shifted ciliary tips, corresponding to arrows. Compared to control, ciliary membrane distribution of ACIII-GFP and MyrPalm-mCherry appears normal in residual cilia of *Bbs1*^{osnKO} OSNs. (*b*) Representative live *en face* images of ectopic (*top*) MyrPalm-mCherry and (*middle*) GFP-tagged cytoplasmic dynein 2 light intermediate chain 1 (Dync2li1-GFP) expression in olfactory epithelium of (*left*) control and (*right*) *Bbs1*^{osnKO} mice. Insets show magnified and color-shifted ciliary tips, corresponding to arrows. Similar to control, Dync2li1-GFP is capable of localizing to tips of *Bbs1*^{osnKO} OSN cilia. Scale bars, 10 μm; 1.25 μm (insets).

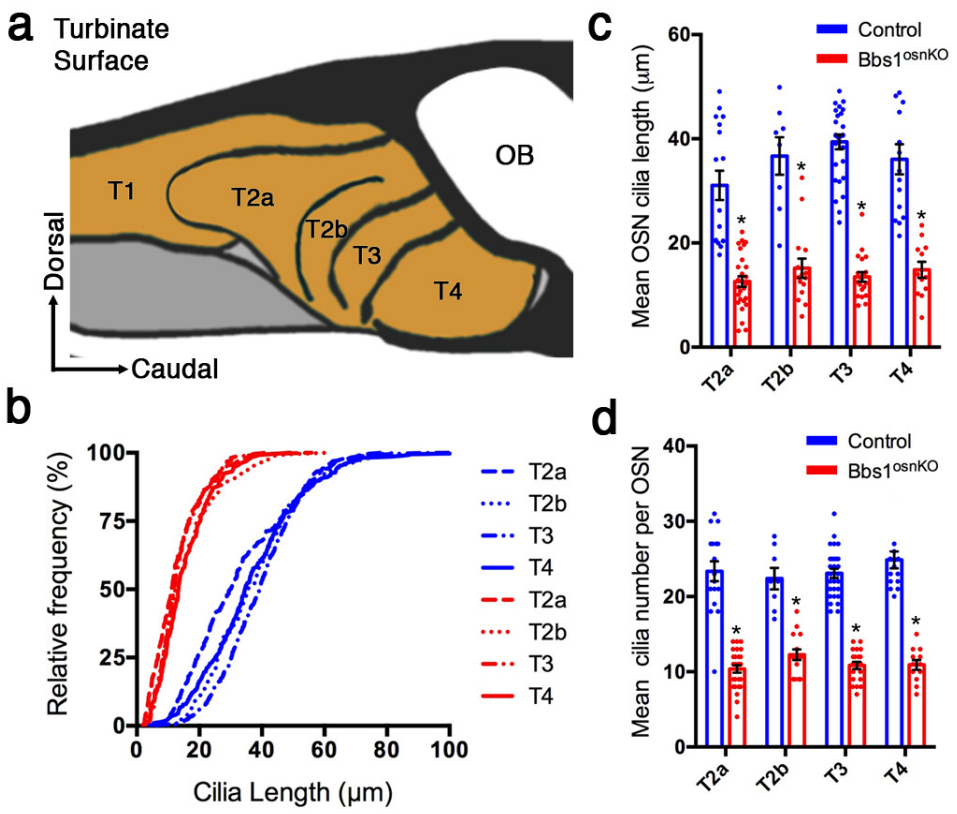

Fig. S3. Uniform olfactory cilia loss across the turbinates OE of *Bbs1*^{osnKO} mutant mice. (*a*) Diagram depicting the regional organization of (*orange*) turbinate olfactory epithelium (TOE) relative to the nasal cavity and olfactory bulb (OB). (*b*) Cumulative distribution of cilia lengths from (*blue*) control and (*red*) *Bbs1*^{osnKO} animals *en face* confocal images from different turbinate regions (control n=1595 cilia on 68 OSNs; *Bbs1*^{osnKO} n=812 cilia on 74 OSNs). (*c*) Quantification of reduced OSN cilia length in (*red*) *Bbs1*^{osnKO} mutants compared to (*blue*) controls, measured from live *en face* confocal images of AV5-mediated ectopically expressed MyrPalm-mCherry in different turbinate regions. Two-Way ANOVA. $F_{(1,134)}$=236.0, *p<0.0001. Post-hoc Bonferroni test. (*d*) Quantification of reduced OSN cilia number in *Bbs1*^{osnKO} mutants. Two-Way ANOVA. $F_{(1,134)}$=396.3, *p<0.0001. Post-hoc Bonferroni test. Values represent means ± SEM.

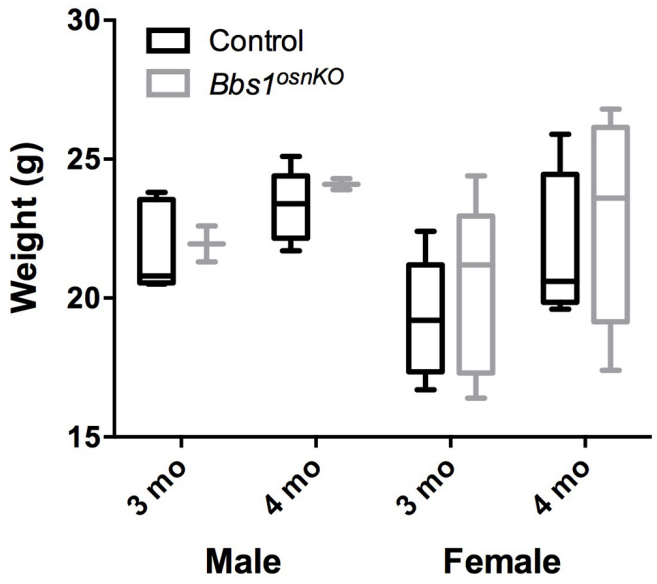

Fig. S4. Olfactory-specific disruption of BBS1 does not induce obesity. *Bbs1*^{osnKO} animals and control littermates were fed *ad libitum* and weighed at three and four months of age. There were no significant differences (Student's t-test, $p>0.05$) between the weights of control and *Bbs1*^{osnKO} mutant (*left*) males or (*right*) females. n=5 control males, 2 *Bbs1*^{osnKO} males, 5 control females, 5 *Bbs1*^{osnKO} females. Values represent means ± SD and min/max.

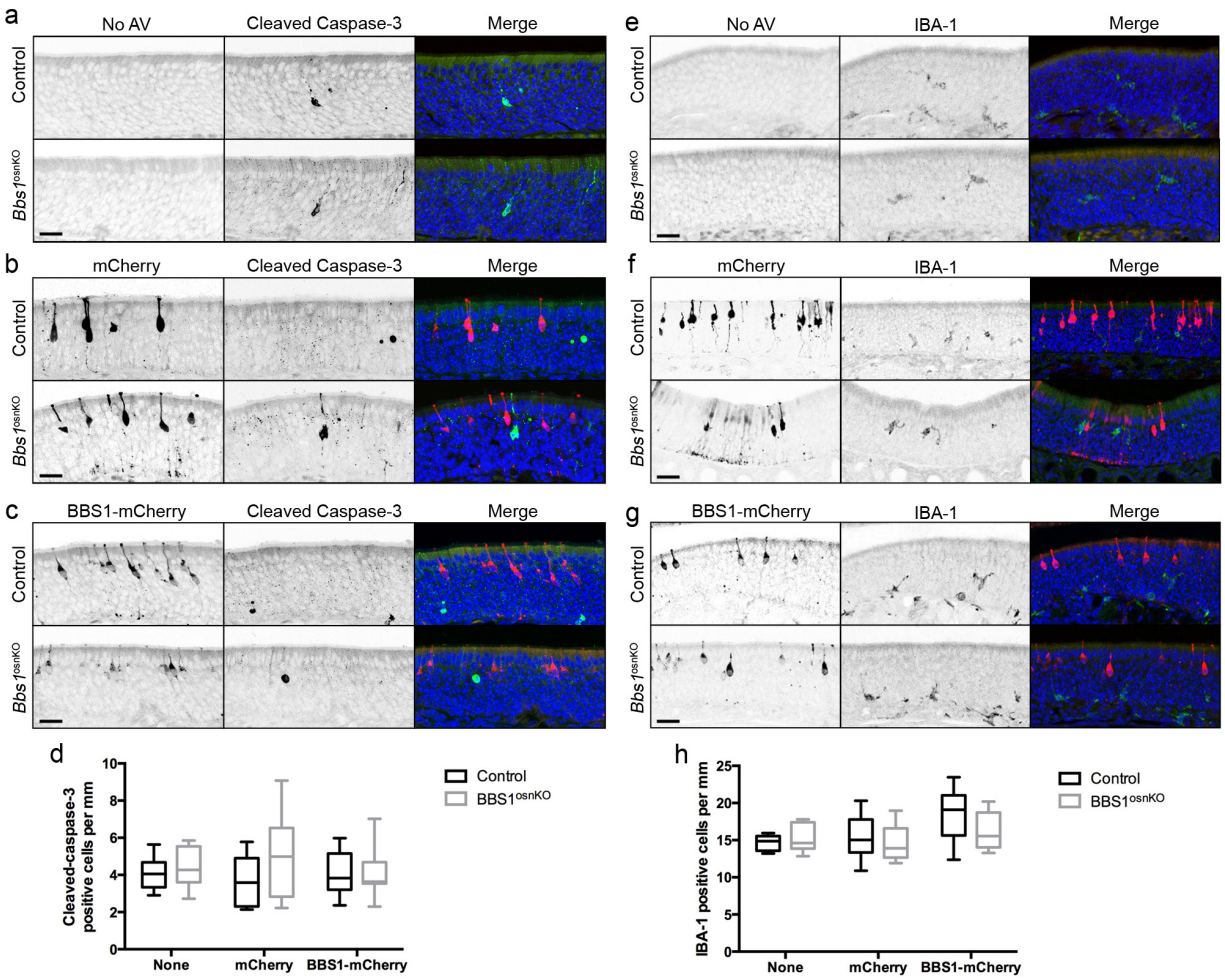
a
No AV
Cleaved Caspase-3
Merge
Control
Bbs1osnKO
b
mCherry
Cleaved Caspase-3
Merge
c
BBS1-mCherry
Cleaved Caspase-3
Merge
e
No AV
IBA-1
Merge
f
mCherry
IBA-1
Merge
g
BBS1-mCherry
IBA-1
Merge
d
Cleaved-caspase-3 positive cells per mm
None
mCherry
BBS1-mCherry
Control
BBS1osnKO
h
IBA-1 positive cells per mm
None
mCherry
BBS1-mCherry
Control
BBS1osnKO

Fig. S5. BBS1 overexpression does not induce apoptosis and macrophage infiltration in the OE. (*a-c*) Representative confocal images of cleaved caspase-3 immunostaining in fixed coronal sections of control and *Bbs1*^{osnKO} mutant OE following (*a*) no treatment, or AV-mediated expression of (*b*) mCherry or (*c*) BBS1-mCherry. (*d*) Quantification of cleaved caspase-3 immunostaining in the OE of untreated control or *Bbs1* osnKO mutants and animals treated with AV-mCherry or AV-BBS1-mCherry. n=3 animals per condition. Student's t-test showed no statistical difference between any groups. (*e-g*) Representative confocal images of IBA-1 immunostaining in fixed coronal sections of control and *Bbs1*^{osnKO} mutant OE following (*e*) no treatment, or AV-mediated expression of (*f*) mCherry or (*g*) BBS1-mCherry. (*h*) Quantification of cleaved caspase-3 immunostaining in the OE of untreated control or *Bbs1* osnKO mutants and animals treated with AV-mCherry or AV-BBS1-mCherry. n=3 animals per condition. Student's t-test showed no statistical difference between any groups. Values represent means ± SD and min/max. Scale bar, 20 μm (*a-c, e-g*).

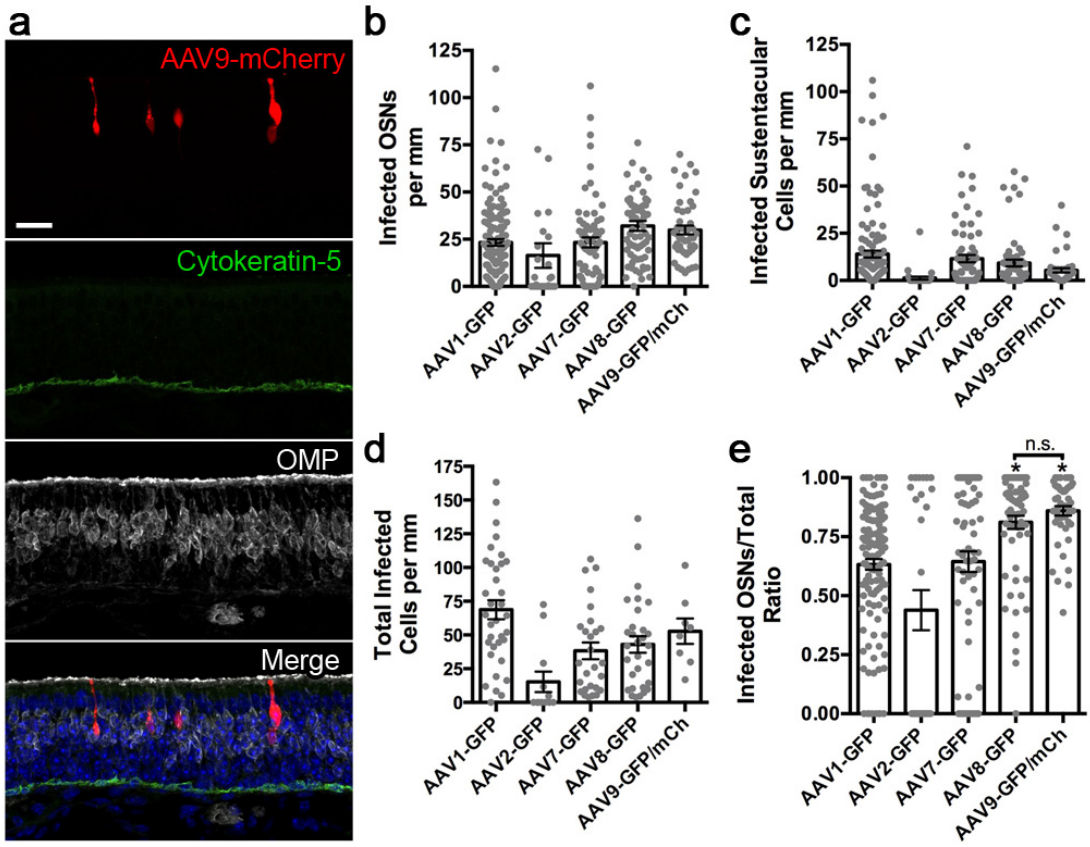

Fig. S6. Adeno-associated viral infection specificity in OE. (*a*) Representative image shows a fixed coronal section of OE from control mice 3 weeks after treatment with AAV9-mCherry. Coronal section was immunostained for cytokeratin-5 to reveal horizontal basal cells and olfactory marker protein (OMP) to reveal mature OSNs. (*b-e*) Quantification of AAV infected (*b*) OSNs, (*c*) sustentacular cells, and (*d*) total cells per mm of OE. (*e*) Quantified data showing changes to the ratio of infected OSNs cells relative to total infected cells on OE surface of control animals across different AAV serotypes. Compared to other AAV serotypes, AAV8 and AAV9-mediated expression show significantly higher relative OSN infection. n = 3 animals per condition. One-way ANOVA, $F_{(4,334)}=14.03$, *p<0.0001, Tukey Post-hoc. Values represent means ± SEM. Scale bar, 20 μm (*a*).